

RESEARCH ARTICLE | *Translational Physiology*

Skeletal muscle LINE-1 retrotransposon activity is upregulated in older versus younger rats

Petey W. Mumford,¹ Matthew A. Romero,¹ Shelby C. Osburn,¹ Paul A. Roberson,¹ Christopher G. Vann,¹ Christopher B. Mobley,² Michael D. Brown,¹ Andreas N. Kavazis,^{1,3} Kaelin C. Young,^{1,3} and Michael D. Roberts^{1,3}

¹School of Kinesiology, Auburn University, Auburn, Alabama; ²Department of Physiology, College of Medicine, University of Kentucky, Lexington, Kentucky; and ³Edward Via College of Osteopathic Medicine, Auburn, Alabama

Submitted 19 April 2019; accepted in final form 11 June 2019

Mumford PW, Romero MA, Osburn SC, Roberson PA, Vann CG, Mobley CB, Brown MD, Kavazis AN, Young KC, Roberts MD. Skeletal muscle LINE-1 retrotransposon activity is upregulated in older versus younger rats. *Am J Physiol Regul Integr Comp Physiol* 317: R397–R406, 2019. First published June 12, 2019; doi:10.1152/ajpregu.00110.2019.—Long interspersed element-1 (LINE-1) is a retrotransposon capable of replicating and inserting LINE-1 copies into the genome. Others have reported skeletal muscle LINE-1 markers are higher in older versus younger mice, but data are lacking in other species. Herein, gastrocnemius muscle from male Fischer 344 rats that were 3, 12, and 24 mo old ($n = 9$ per group) were analyzed for LINE-1 mRNA, DNA, promoter methylation and DNA accessibility. qPCR primers were designed for active (L1.3) and inactive (L1.Tot) LINE-1 elements as well as part of the ORF1 sequence. L1.3, L1.Tot, and ORF1 mRNAs were higher ($P < 0.05$) in 12/24 versus 3-mo-old rats. L1.3 DNA was higher in the 24-mo-old rats versus other groups, and ORF1 DNA was greater in 12/24 versus 3-mo-old rats. ORF1 protein was higher in 12/24 versus 3-mo-old rats. RNA-sequencing indicated mRNAs related to DNA methylation (*Tet1*) and histone acetylation (*Hdac2*) were lower in 24 versus 3-mo-old rats. L1.3 DNA accessibility was higher in 24-mo-old versus 3-mo-old rats. No age-related differences in nuclear histone deacetylase (HDAC) activity existed, although nuclear DNA methyltransferase (DNMT) activity was lower in 12/24 versus 3-mo-old rats ($P < 0.05$). In summary, markers of skeletal muscle LINE-1 activity increase across the age spectrum of rats, and this may be related to deficits in DNMT activity and/or increased LINE-1 DNA accessibility.

aging; LINE-1; retrotransposons; skeletal muscle

INTRODUCTION

The long interspersed element-1 (LINE-1) is a class I transposable element, and repeats of this gene account for ~18% of mice DNA (54), 23% of rat DNA (13), and 17% of human DNA (24). While a majority of genomic LINE-1 copies are considered inactive due to either rearrangement, point mutations, or truncations, there are roughly 3,000 LINE-1 copies in mice, and 500 LINE-1 copies in rats, and 100 active LINE-1 copies in humans which are retrotransposition-competent (3, 14, 41). In this regard, LINE-1 is commonly referred to as a jumping gene given that active elements have the ability to be

transcribed and be pasted back into the genome via autonomous retrotransposition.

A full-length retrotransposition-competent LINE-1 copy is ~6 to 6.5 kilobases long and consists of a 5' untranslated region (UTR), two open reading frames (ORF1 and ORF2) followed by a 3'-UTR (44). ORF1 encodes a 40 kDa RNA binding protein that preferentially binds to LINE-1 mRNA in trimers to aid in translocation of the LINE-1 mRNA back into the nucleus (32), while ORF2 encodes a 150-kDa protein that possesses endonuclease (10) and reverse transcriptase domains (34). LINE-1 retrotransposition begins with the recruitment of RNA polymerase II to the endogenous LINE-1 promoter and subsequent transcription. Once transcribed, LINE-1 mRNA is transported into the cytoplasm where it is translated into the ORF1p and ORF2p proteins (termed ORF1 and ORF2 proteins, hereafter). Both ORF1 and ORF2 proteins preferentially bind to LINE-1 mRNA, forming a ribonucleoprotein particle (RNP) (9, 18, 31, 55). After RNP formation, the complex is capable of translocating back into the nucleus. The ORF2 protein on the RNP nicks genomic DNA and uses a free 3' hydroxyl group to prime reverse transcription (7). This process is deemed target-primed reverse transcription (TPRT) (28) and appears to be random in that de novo LINE-1 insertions can occur in promoter/regulatory regions, or introns and exon sequences to affect gene expression (4). TPRT is not completely efficient, and the premature termination of the TPRT process can occur through inhibitory mechanisms resulting in truncated LINE-1 gene fragments within the genome (12).

Skeletal muscle aging is associated with epigenetic alterations, mitochondrial dysfunction, cellular senescence, and atrophy (21, 25, 27). Furthermore, fiber type conversion (17, 20, 26, 38, 47), a decline in myosin heavy chain mRNA (1, 2, 5, 33, 48), and a decline in contractile (or myofibrillar) protein content (15) have all been reported in skeletal muscle from older versus younger humans or rodents. Interestingly, only one paper published to date has demonstrated LINE-1 mRNA expression and DNA copy number increases with age in skeletal muscle of mice (8). While the phenotypic consequences of increased skeletal muscle LINE-1 were not elucidated, a recent study reported global Sirt6-knockout mice exhibit a severe premature aging phenotype driven through enhanced LINE-1 mRNA expression and retrotransposition (53). Simon et al. (49) also recently reported that hind limb muscle masses as well as quadriceps muscle fiber diameters were significantly lower in Sirt6-knockout compared with

Address for reprint requests and other correspondence: M. D. Roberts, School of Kinesiology, Molecular and Applied Sciences Laboratory, Auburn University, 301 Wire Rd., Office 286, Auburn, AL 36849 (e-mail: mdr0024@auburn.edu).

wild-type mice. Notwithstanding, the cause of increased skeletal muscle LINE-1 mRNA and DNA content with aging has not been well elucidated, and it also remains to be determined whether this phenomenon is observed across species. Therefore, the primary purpose of this investigation was to determine whether aging affects both LINE-1 mRNA expression and LINE-1 DNA content in rat skeletal muscle tissue. We also sought to examine how skeletal muscle LINE-1 5'-UTR promoter methylation and LINE-1 DNA accessibility are impacted by aging in rats. We hypothesized that markers of increased LINE-1 activity would be elevated in older versus younger rats, and this would be due to either alterations in LINE-1 5'-UTR promoter methylation and/or DNA accessibility.

MATERIALS AND METHODS

Animals

All animal experimental procedures were approved by Auburn University's Institutional Animal Care and Use Committee. Fischer 344 male rats aged 3, 12, and 24 mo ($n = 9$ per age group) were purchased via Envigo Laboratories (Indianapolis, IN). Rats were housed two per cage at the Auburn University Biological Research Facility in quarters with constant 12-h light and 12-h dark cycles at ambient room temperature. Standard chow (24% protein, 58% carbohydrate, 18% fat; Teklad Global no. 2018 Diet, Envigo Laboratories) and tap water were provided to animals ad libitum.

The morning of the necropsies, rats were removed from the Biological Research Facility, transported to the Molecular and Applied Sciences Laboratory in the School of Kinesiology, and were then acclimated for ~3–4 h with ad libitum access to water only. After acclimation, rats were euthanized under CO₂ gas induction in a 2-liter chamber (VetEquip, Pleasanton, CA). Thereafter, total body mass was recorded, and right-leg gastrocnemius muscle was dissected out and weighed using an analytical scale with a sensitivity of 0.0001 g (Mettler-Toledo; Columbus, OH). Dissections on the right-leg gastrocnemius muscle were performed close to the origin and insertion sites, and any visible connective or fat tissue was removed. Tissues were then flash frozen in liquid nitrogen and stored at -80°C until analyses, described below.

Tissue Preparation for Protein Analyses

Mixed gastrocnemius tissues were removed from -80°C storage, tissue was crushed on a liquid nitrogen-cooled mortar and pestle, and ~50 mg of tissue from each rodent were placed in 500 μl of ice-cold general cell lysis buffer [20 mM Tris HCl (pH 7.5), 150 mM NaCl, 1 mM sodium-EDTA, 1 mM EGTA, 1% Triton, 20 mM sodium pyrophosphate, 25 mM sodium fluoride, 1 mM β -glycerophosphate, 1 mM Na₃VO₄ and 1 $\mu\text{g}/\text{ml}$ leupeptin] (Cell Signaling; Danvers, MA). Tissues were homogenized via micro pestles and homogenates were centrifuged at 500 g for 5 min. After centrifugation insoluble proteins were removed and supernatants were stored at -80°C before Western blot analysis.

Western Blot Analysis

Total protein determination on supernatants were performed following the dye-based bicinchoninic acid (BCA) colorimetric assay (Thermo Fischer Scientific, Waltham, MA). Supernatants were subsequently prepared for SDS-PAGE using 4 \times Laemmli buffer at 2 $\mu\text{g}/\mu\text{l}$, and 15 μl were loaded onto 4–15% SDS-polyacrylamide precasted gels (Bio-Rad Laboratories; Hercules, CA). 1 \times SDS-PAGE run buffer (Amersco; Framingham, MA) was used for electrophoresis at 180 V for 60 min. Thereafter, proteins were transferred to polyvinylidene difluoride membranes (Bio-Rad Laboratories) via con-

stant amperage (200 mA) for 120 min. Membranes were then stained with Ponceau S and digital images were captured using a gel documentation system (UVP, Upland, CA) to ensure equal loading of samples between lanes. Membranes were then blocked at room temperature with 5% nonfat milk powder in Tris-buffered saline with 0.1% Tween-20 (TBST) for 1 hour. All following primary antibodies were incubated overnight at 4°C in a solution of TBST containing 5% BSA (Amersco): 1) mouse anti-ORF1 (1:1,000, cat. no. ab76726, Abcam, Cambridge, MA), 2) rabbit anti-DNMT3A (1:1,000, cat. no. 2160S, Cell Signaling), 3) rabbit anti-TET1 (1:1,000, cat. no. ab191698, Abcam), 4) rabbit anti-histone deacetylase (HDAC2) (1:1,000, cat. no. 2540, Cell Signaling), and 5) rabbit anti-CTCF protein (1:1,000, cat. no. 2899, Cell Signaling). The following day, membranes were incubated with HRP-conjugated anti-mouse or anti-rabbit IgG secondary antibodies (1:2,000; Cell Signaling) in a solution of TBST containing 5% BSA at room temperature for 1 h. Thereafter, membranes were developed using an enhanced chemiluminescent reagent (Luminata Forte HRP substrate; EMD Millipore, Billerica, MA) where band densitometry was assessed by use of a digital gel documentation system and associated densitometry software (UVP). Densitometric values of white bands for each target were normalized to dark band Ponceau densitometry values. These values were then normalized to the 3-mo group average to yield relative expression units (REUs).

RNA Isolation, cDNA Synthesis, and RT-PCR

Approximately 20 mg of frozen mixed gastrocnemius muscle from each rodent were placed in 500 μl of Ribozol (Amersco, Solon, OH) per the manufacturer's recommendations. Thereafter, phase separation was achieved according to manufacturer's instructions for RNA isolation. Following RNA precipitation and pelleting, pellets were resuspended in 30 μl of RNase-free water, and RNA concentrations were determined in duplicate at an absorbance of 260 nm by using a NanoDrop Lite (Thermo Fisher Scientific). cDNA (2 μg) was synthesized using a commercial qScript cDNA SuperMix (Quanta Biosciences, Gaithersburg, MD) per the manufacturer's recommendations. RT-PCR was performed with gene-specific primers and SYBR-green-based methods in a RT-PCR thermal cycler (Bio-Rad). Primers were designed with primer designer software (Primer3Plus, Cambridge, MA), and melt curve analyses demonstrated that one PCR product was amplified per reaction. Additionally, PCR products were resolved on 1% agarose gels to verify that a product produced at the anticipated molecular weight was obtained. Three primer sets were designed to interrogate LINE-1 mRNA and DNA expression. The first primer set (L1.3) amplified a portion of the 5'-UTR region and was designed to probe for the most active LINE-1 element based upon the findings of Kirilyuk et al. (23). The second primer set (L1.Tot) also amplified a portion of the 5'-UTR region and was designed to encompass full-length LINE-1 elements that contained a 5' promoter, but did not have the ability to undergo retrotransposition based on mutations in the protein coding regions (23). We also designed a primer set to amplify a portion of the ORF1 region. The forward and reverse primer sequences for all genes are listed in Table 1. Fold change values from 3-mo-old rats were performed using the $2^{\Delta\Delta\text{Cq}}$ method where $2^{\Delta\text{Cq}} = 2^{\Delta[\text{housekeeping gene (HKG) Cq} - \text{gene of interest Cq}]}$ and $2^{\Delta\Delta\text{Cq}}$ (or fold change) = $[2^{\Delta\text{Cq}} \text{ value} / 2^{\Delta\text{Cq}} \text{ average of 3 mo age group}]$. The geometric mean of fibrillarlin (*Fbl*), glyceraldehyde 3-phosphate dehydrogenase (*Gapdh*), cyclophilin A (*Ppia*), and hypoxanthine phosphoribosyltransferase 1 (*Hprt1*) was used to normalize mRNA expression results. While data are represented as fold change from the 3-mo group, they are presented as REUs. The overall coefficient of variation values for Cq duplicates of the assayed genes were as follows: HKG = 0.99%, L1.3 = 0.47%, L1.Tot = 0.53%, ORF1 = 0.43%.

Table 1. Rat primer sequences used for real-time PCR

Gene	Accession No.	Amplicon Length
Glyceraldehyde-3-phosphate dehydrogenase (<i>Gapdh</i> ; HKG) FP (5' → 3'): TGATGCCCCCATGTTTGTGA RP (5' → 3'): GGCATGGACTGTGGTCATGA	NM_017008.4	163 bp
Fibrillarin (<i>Fbl</i> ; HKG) FP (5' → 3'): CTGCGGAATGGAGGACACTT RP (5' → 3'): GATGCAAACACAGCCTCTGC	NM_001025643.1	83 bp
Cyclophilin A (<i>Ppia</i> ; HKG) FP (5' → 3'): GCATACAGGTCCTGGCCTCT RP (5' → 3'): AGCCACTCAGTCTTGGCAGT	NM_017101.1	93 bp
Hypoxanthine phosphoribosyltransferase 1 (<i>Hprt1</i> ; HKG) FP (5' → 3'): AAGACAGCGGCAAGTTGAAT RP (5' → 3'): GGGCCTGTGTCTTGAGTTCA	NM_012583.2	192 bp
Ribosomal protein S16 (<i>Rps16</i> ; HKG) FP (5' → 3'): TCGCTGCGAATCCAAGAAGT RP (5' → 3'): CCCTGATCCTTGAGACTGGC	NM_001169146.1	87 bp
Histone deacetylase 1 (<i>Hdac1</i> ; HKG) FP (5' → 3'): GAGCGGTGATGAGGATGAGG RP (5' → 3'): CACAGGCAATGCGTTTGTCA	NM_001025409.1	74 bp
β 2-Microglobulin (<i>B2m</i> ; HKG) FP (5' → 3'): GGAAACTGAGGGGAGTAGGG RP (5' → 3'): CCTGGGCTTTCATCCTAACA	NM_012512.2	143 bp
LINE-1 5'-UTR primer set 1 (L1.3) FP (5' → 3'): GACCATCTGGAACCCTGGTG RP (5' → 3'): GGGCCTGTGTCTTGAGTTCA	DQ100473.1	181 bp
LINE-1 5'-UTR primer set 2 (L1.Tot) FP (5' → 3'): GGAAGAGACCACCAACTG RP (5' → 3'): GAAGGTTTAGCTCTCCCTCC	DQ100473.1 DQ100475.1 DQ100476.1 DQ100477.1 DQ100474.1 DQ100482.1	200 bp
LINE-1 Open Reading Frame 1 (ORF1) FP (5' → 3'): AAGAAACACCTCCCGTCACA RP (5' → 3'): CCTCCTTATGTTGGGCTTACC	N/A	N/A

bp, base pairs; LINE-1, long interspersed element-1; HKG, housekeeping gene; 5'-UTR, 5' untranslated region.

DNA Isolation and RT-PCR for Assessing LINE-1 DNA Content

Mixed gastrocnemius was removed from -80°C , and ~ 25 mg of each tissue from each rodent were processed using the commercially available DNA isolation kit DNeasy Blood & Tissue Kit (Qiagen, Venlo, The Netherlands) per the manufacturer's recommendations. Following DNA precipitation and pelleting, pellets were resuspended in 200 μl elution buffer from the kit, and DNA concentrations were determined in duplicate at an absorbance of 260 nm using a NanoDrop Lite (Thermo Fisher Scientific). DNA (25 ng) was subjected to RT-PCR analysis using the aforementioned methods. The geometric-mean of ribosomal protein S16 (*Rps16*), histone deacetylase 1 (*Hdac1*), and β 2-microglobulin (*B2m*) was used to normalize DNA expression results. Fold change values from 3-mo-old rats were performed using the aforementioned $2^{\Delta\Delta\text{Cq}}$ method, and data are presented as REUs. Overall coefficient of variation values for Cq duplicates of the assayed genes were as follows: L1.3 = 0.51% and L1.Tot = 0.62%, ORF1 = 0.31%, HKG = 0.24%.

LINE-1 5'-UTR Promoter Methylation Analysis

LINE-1 5'-UTR promoter methylation analysis was performed on isolated gastrocnemius DNA (described above) from $n = 8$ rats per age group using a commercially available methylated DNA immunoprecipitation (MeDIP) kit (product no. ab117133; Abcam). Before the assay as performed, 1.5 μg of gastrocnemius DNA was digested using MseI (New England BioLabs, Ipswich, MA). Following digestion reactions, total methylated DNA from a total of 1 μg input was immunoprecipitated using an anti-5-methylcytosine antibody provided within the kit. RT-PCR was then performed on 25 ng of the methylated DNA using the L1.3 primers described above to decipher

fold change in methylated LINE-1 5'-UTR. Residual input DNA from each sample (25 ng) was used as a control to normalize RT-PCR results. Fold change in 5-UTR promoter methylation was calculated using the $2^{\Delta\Delta\text{Cq}}$ method where $2^{\Delta\text{Cq}} = 2^{\Delta[\text{input L1.3 DNA Cq} - \text{methylated L1.3 DNA Cq}]}$ (or fold change) = $[2^{\Delta\text{Cq}} \text{ value}/2^{\Delta\text{Cq}} \text{ average of 3 mo age group}]$. Fold change values from 3-mo-old rats were performed using the aforementioned $2^{\Delta\Delta\text{Cq}}$ method, and data are presented as REUs. Overall coefficient of variation values for Cq triplicates of the assayed genes were as follows: input L1.3 = 0.44% and methylated L1.3 = 0.35%.

LINE-1 Chromatin Accessibility Analysis

LINE-1 chromatin accessibility was assessed from $n = 8$ rats per age group using a commercially available kit (Chromatin Accessibility Assay Kit, product no. ab185901; Abcam) per the manufacturer's recommendations. Briefly, methods involved obtaining DNA, digesting the DNA using a proprietary nuclear digestion buffer, and performing RT-PCR on digested versus undigested samples. The premise of the assay operates through a gene of interest localized to euchromatin regions being more susceptible to digestion and, thus, possessing a lower RT-PCR amplification signal relative to genes in heterochromatin regions. RT-PCR was performed on 25 ng of digested DNA using the L1.3 primers described above to decipher fold change in genomic LINE-1 residing in euchromatin. Undigested DNA from each sample (25 ng) was used as a control to normalize RT-PCR results. Fold change in L1.3 euchromatin DNA was calculated using the $2^{\Delta\Delta\text{Cq}}$ method where $2^{\Delta\text{Cq}} = 2^{\Delta[\text{digested L1.3 DNA Cq} - \text{undigested L1.3 DNA Cq}]}$ and $2^{\Delta\Delta\text{Cq}}$ (or fold change) = $[2^{\Delta\text{Cq}} \text{ value}/2^{\Delta\text{Cq}} \text{ average of 3-mo age group}]$. Fold change values from 3-mo-old rats

were performed using the aforementioned $2^{\Delta\Delta C_q}$ method, and data are presented as REUs. Overall coefficient of variation values for Cq triplicates of the assayed genes were as follows: undigested L1.3 DNA = 1.64% and digested L1.3 DNA = 0.36%.

DNA Methyltransferase Activity Assay

Before assaying DNA methyltransferase (DNMT) activity, nuclear protein extraction was performed on frozen gastrocnemius muscle (~25 mg) using a commercially available kit (Nuclear Extraction Kit; Abcam) per the manufacturer's recommendations. Global DNMT activity of nuclear isolates (10 μ l) was assessed using a commercially available kit (DNMT Activity Assay Kit, no. ab113467, Abcam) per the manufacturer's recommendations. DNMT activity was expressed as REUs, which were then normalized to input muscle weights. Overall coefficient of variation values for duplicate readings were 33.2%.

HDAC Activity Assay

Global HDAC activity on nuclear isolates (10 μ l) was assessed using a commercially available fluorometric kit (Histone Deacetylase Activity Assay Kit, no. ab156064, Abcam,) per the manufacturer's recommendations. HDAC activity was expressed as relative fluorescence units, which were then normalized to input muscle weights. Overall coefficient of variation values for duplicate readings were 5.3%.

RNA-sequencing

RNA-sequencing was performed only on a subset of 3-mo ($n = 8$) and 24-mo ($n = 8$) with the intent of identifying how aging affected the mRNA expression of genes related to LINE-1 regulation. Gastrocnemius tissues were processed for RNA isolation using methods described above. Thereafter, RNA was shipped to LC Sciences (Houston, TX) for RNA-sequencing. The steps described below were completed for this analysis.

Library preparation and sequencing. Total RNA quality and quantity were assessed using Bioanalyzer 2100 and RNA 6000 Nano LabChip Kits (Agilent Technologies, Santa Clara, CA). Total RNA was subjected to poly(A) mRNA enrichment with poly-T oligo-attached magnetic beads (Invitrogen). Following purification, the poly(A) mRNA fractions were fragmented into small pieces using divalent cations under elevated temperature. The cleaved RNA fragments were subsequently reverse-transcribed to create final cDNA libraries in accordance with strand-specific library preparation by dUTP method. The average insert size for the paired-end libraries was 300 ± 50 bp. Paired-end 2×150 base pair sequencing was performed on an Illumina HiSeq 4000 platform following the manufacturer's recommended protocol.

Transcripts assembly. Cutadapt (30) and perl scripts were used to remove the reads that contained adaptor contamination, low quality bases, and undetermined bases. Sequence quality was verified using FastQC (<http://www.bioinformatics.babraham.ac.uk/projects/fastqc/>). HISAT2 (22) was used to map reads to the genome of *Rattus norvegicus* (version: v88). The mapped reads of each sample were assembled using StringTie (42). Thereafter, all transcriptomes from the 16 samples were merged to reconstruct a comprehensive transcriptome using perl scripts and gffcompare (<https://github.com/gperteau/gffcompare/>). After the final transcriptome was generated, StringTie (42) and Ballgown (11) were used to estimate the expression levels of all transcripts.

Differential expression analysis of mRNAs. StringTie (42) was used to measure expression levels for mRNAs by calculating FPKM values $\{FPKM = [\text{total_exon_fragments}/\text{mapped_reads}(\text{millions}) \times \text{exon_length}(\text{kB})]\}$. Differentially expressed transcripts related to LINE-1 regulation between the young and old groups were determined by comparing FPKM values. Given that RNA sequencing was used as a screening tool herein, differentially expressed transcripts related to LINE-1 regulation were considered meaningful if the unadjusted P value of a given mRNA between groups was $P < 0.05$.

Age-Related Skeletal Muscle Phenotyping

Beyond examining skeletal muscle LINE-1 pathway markers in the three cohorts, we also sought to analyze muscle for age-related phenotypes. These methods are described below.

Total myofibrillar protein assessment. Myofibrillar protein isolations were performed based on the methods of Goldberg's laboratory (6). Briefly, mixed gastrocnemius foils were removed from -80°C storage, tissue was crushed on a liquid nitrogen-cooled mortar and pestle, muscle (~20 mg) was weighed using an analytical scale sensitive to 0.0001 g (Mettler-Toledo, Columbus, OH) and immediately placed in 1.7 ml polypropylene tubes containing 190 μ l of ice-cold homogenizing buffer (20 mM Tris HCl, pH 7.2, 5 mM EGTA, 100 mM KCl, 1% Triton X-100) and 6.4 M spermidine (Alfa Aesar, Haverhill, MA). Samples were homogenized on ice using tight-fitting pestles, and centrifuged at 3,000 g for 30 min at 4°C . The resultant pellet was resuspended in homogenizing buffer, and samples were centrifuged at 3,000 g for 10 min at 4°C . Resultant supernatants from this step were discarded, resultant pellets were resuspended in 190 μ l ice-cold wash buffer (20 mM Tris HCl, pH 7.2, 100 mM KCl, 1 mM DTT), and samples were centrifuged at 3,000 g for 10 min at 4°C ; this specific process was performed twice. Final myofibril pellets were resuspended in 200 μ l of ice-cold storage buffer (20 mM Tris-HCl, pH 7.2, 100 mM KCl, 20% glycerol, 1 mM DTT) and frozen at -80°C until protein

Table 2. Effects of age group on skeletal muscle characteristics

	Age Group, months old			ANOVA		
	3	12	24	F	P	η_p^2
Body mass, g*	285 \pm 29 ^b	429 \pm 20 ^a	439 \pm 42 ^a	73.73	<0.001	0.86
Gastroc. mass, g†	1.21 \pm 0.11 ^c	1.57 \pm 0.08 ^a	1.45 \pm 0.08 ^b	35.51	<0.001	0.75
Relative gastroc. mass, mg/g†	4.31 \pm 0.28 ^a	3.67 \pm 0.18 ^b	3.32 \pm 0.19 ^c	52.04	<0.001	0.81
Myofibrillar protein, μ g/mg wet muscle	78.34 \pm 7.08	76.63 \pm 7.21	78.12 \pm 5.14	0.20	= 0.818	0.02
Myosin protein, ADU/mg wet muscle	1.71 \pm 0.28	1.67 \pm 0.30	1.60 \pm 0.34	0.35	= 0.711	0.03
Actin protein, ADU/mg wet muscle	1.07 \pm 0.16	1.17 \pm 0.14	1.18 \pm 0.15	1.33	= 0.284	0.10
CS activity, mM \cdot min ⁻¹ \cdot mg protein ⁻¹	0.23 \pm 0.03	0.24 \pm 0.05	0.21 \pm 0.03	1.04	= 0.369	0.08
Muscle triglycerides, μ mol/g wet muscle	1.62 \pm 0.48	1.57 \pm 0.32	1.61 \pm 0.44	0.05	= 0.955	0.01

Data are expressed as means \pm SD ($n = 8$ rats per group). The F and P values are reported from one-way ANOVAs, including age as the between-subjects factor. Gastroc, gastrocnemius; ADU, arbitrary density units; CS, citrate synthase. ^aSignificant between age group differences ($P < 0.05$). ^bSignificant between age group differences ($P < 0.05$). ^cSignificant between age group differences ($P < 0.05$). *These data were published by Mobley et al. (37). †These data were published by Mumford et al. (39) and are presented here for the convenience of the reader.

concentration determination. Myofibrillar protein concentrations were determined using a BCA assay, which were then normalized to input muscle weights. Overall coefficient of variation values for triplicate readings were 2.04%.

Determination of myosin heavy chain and actin content. SDS-PAGE preps from resuspended myofibrils were performed using: 1) 10 μ l resuspended myofibrils, 2) 65 μ l distilled water (dH_2O), and 3) 25 μ l 4 \times Laemmli buffer. Samples (5 μ l) were then loaded on precasted gradient (4–15%) SDS-polyacrylamide gels (Bio-Rad Laboratories) and subjected to electrophoresis (200 V for 45 min) using premade 1 \times SDS-PAGE running buffer (Amersco). After electrophoresis gels were rinsed in dH_2O for 15 min and immersed in Coomassie stain (LabSafe GEL Blue; G-Biosciences, St. Louis, MO) for 45 min. Thereafter, gels were destained in dH_2O for 60 min, bright-field imaged using a gel documentation system (UVP), and band densities were determined using associated software. Myosin and actin concentrations were expressed as arbitrary density units (ADU) per milligram muscle, and this assay was performed in singlets due to its robust sensitivity (45).

Citrate synthase activity assay. Mixed gastrocnemius foils were removed from -80°C storage, tissue was crushed on a liquid nitrogen-cooled mortar and pestle, and ~ 30 mg of tissue from each rodent were placed in 500 μ l of ice-cold cell lysis buffer (recipe described above) (Cell Signaling). Tissues were homogenized via micro pestles

and homogenates were centrifuged at 500 g for 5 min. After centrifugation, insoluble proteins were removed, and supernatants were stored at -80°C before citrate synthase activity assessments. Citrate synthase activity was as previously described by our laboratory (19). The assay principle is based upon the reduction of 5,5-dithiobis (2-nitrobenzoic acid) (DTNB) at 412 nm (extinction coefficient 13.6 $\text{mmol}\cdot\text{l}^{-1}\cdot\text{cm}^{-1}$) coupled to the reduction of acetyl-CoA by the citrate synthase reaction in the presence of oxaloacetate. Briefly, 2 μ g of skeletal muscle protein was added to a mixture composed of 0.125 mol/l Tris-HCl (pH 8.0), 0.03 mmol/l acetyl-CoA, and 0.1 mmol/l DTNB. The reaction was initiated by the addition of 5 μ l of 50 mmol/l oxaloacetate and the absorbance change was recorded for 1 min. Overall coefficient of variation values for duplicate readings were 4.2%.

Muscle triglyceride assay. Gastrocnemius skeletal muscle tissue (~ 20 mg) was weighed using an analytical scale sensitive to 0.0001 g (Mettler-Toledo, Columbus, OH), and immediately placed in 1.7 ml polypropylene tubes. Thereafter, triglyceride analysis was performed using a commercially available triglyceride colorimetric kit (Cayman Chemical, Ann Arbor, MI) according to manufacturer's instructions. Gastrocnemius skeletal muscle triglyceride content was expressed μmol per gram wet muscle. Overall coefficient of variation values for duplicate readings were 1.2%.

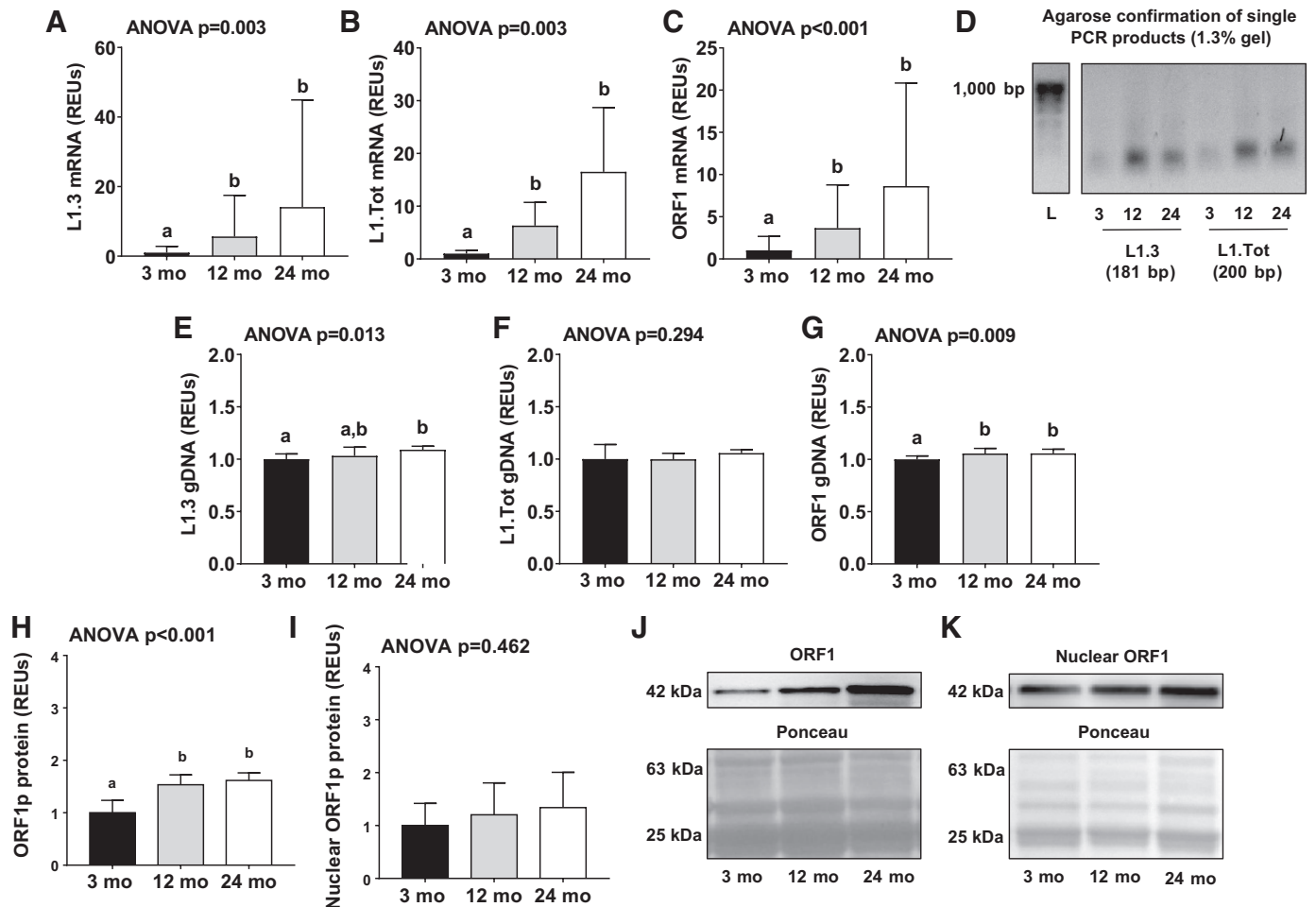


Fig. 1. Effect of aging on skeletal muscle long interspersed element-1 (LINE-1) mRNA, DNA, and protein expression. Age group differences are shown in L1.3 mRNA (A), L1.Tot mRNA (B), and ORF1 mRNA (C). Right panels in A, B, and C include \log_{10} transformed individual data from each rat. D: L1.3 and L1.Tot primer validation through agarose gel electrophoresis. E: age group differences in L1.3 DNA content (gDNA). F: L1.Tot DNA content. G: ORF1 DNA content. H: total ORF1 protein expression. I: nuclear ORF1 protein expression. Data are means \pm SD ($n = 9$ rats per group). ^{a,b}Significant between-group age differences ($P < 0.05$). L: 50 bp DNA ladder. J and K: total and nuclear ORF1 representative Western blot images.

Statistical Analyses

Statistics were performed using the open-source software R (42a), R Studio (46a), and SPSS v 23.0 (IBM, Armonk, NY). Before statistical analysis, assumption testing was performed on all dependent variables. For non-normally distributed data, values were log-transformed and reanalyzed for normality. Dependent variables for the rodent experiments were analyzed using one-way ANOVAs with Fisher LSD post hoc tests or Welch's *t*-tests (when assumptions were violated) to assess differences in dependent variables between age groups. Magnitude of effects are also expressed in the results using partial eta squared (η_p^2) effect size, and effect sizes of 0.01, 0.06 and >0.14 were considered small, moderate, and large, respectively. Statistical significance for all null hypothesis testing was set at $P < 0.05$. All data herein is presented as means \pm SD.

RESULTS

Skeletal Muscle Mass, Myofibrillar Protein, Citrate Synthase, Collagen, and Triglyceride Levels

Table 2 contains data related to skeletal muscle aging phenotype. Notably, body masses and gastrocnemius masses from these rats have been previously reported (37, 39). There were no significant between-group differences for myofibrillar protein concentrations, myosin protein concentrations, actin protein concentrations, citrate synthase activity or muscle triglyceride concentrations.

Gastrocnemius LINE-1 Activity Markers

L1.3, L1.Tot, and ORF1 mRNA expression were not normally distributed, and these variables were log-transformed before statistical analysis. L1.3 mRNA expression was significantly different between age groups ($P = 0.003$, $\eta_p^2 = 0.38$; Fig. 1A), and post hoc analysis revealed that 12-mo-old and 24-mo-old rats had higher L1.3 mRNA expression compared with 3-mo-old rats ($P < 0.05$). L1.Tot mRNA expression was significantly different between age groups ($P = 0.003$, $\eta_p^2 = 0.42$; Fig. 1B), and post hoc analysis revealed that 12-mo and 24-mo rats had higher L1.3 mRNA expression compared with 3-mo rats ($P < 0.05$). ORF1 mRNA expression was significantly different between age groups ($P < 0.001$, $\eta_p^2 = 0.47$; Fig. 1C), and post hoc analysis revealed that 12-mo and 24-mo rats had higher ORF1 RNA expression compared with 3-mo rats ($P < 0.05$).

L1.3 DNA content was significantly different between age groups ($P = 0.013$, $\eta_p^2 = 0.31$; Fig. 1E), and post hoc analysis revealed that 24-mo-old rats had higher expression levels compared with 3-mo-old rats ($P < 0.05$). ORF1 DNA content was significantly different between age groups ($P = 0.009$, $\eta_p^2 = 0.33$; Fig. 1G), and post hoc analysis revealed that both 12-mo and 24-mo-old rats had higher expression compared with 3-mo-old rats ($P < 0.05$). Total ORF1 protein expression was significantly different between age groups ($P < 0.001$,

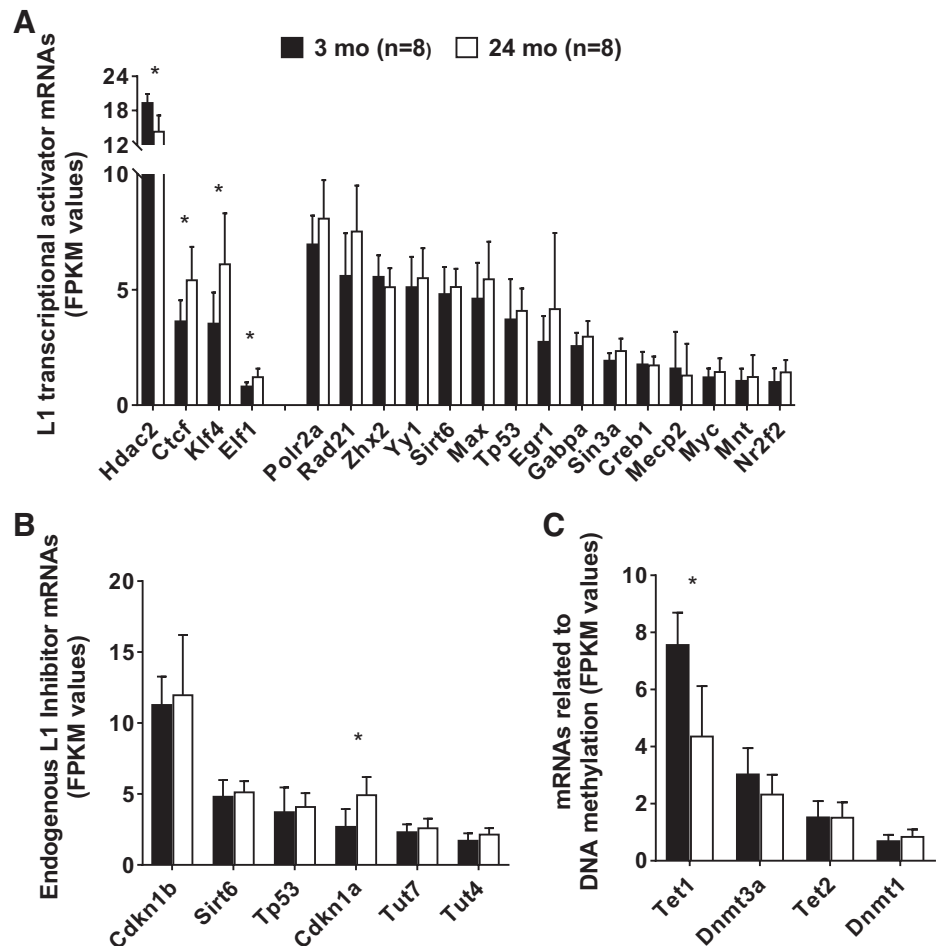


Fig. 2. Muscle RNA-sequencing results for 3-month-old and 24-month-old rats. Age group differences are shown in long interspersed element-1 (LINE-1) transcriptional activators (A), LINE-1 endogenous inhibitors (B), and genes related to DNA methylation (C). FPKM, [total_exon_fragments/mapped_reads(millions) \times exon_length(kB)]. Data are presented as means \pm SD ($n = 8$ per group). *Significant between-group age differences ($P < 0.05$).

$\eta_p^2 = 0.69$; Fig. 1H), and post hoc analysis revealed that 12-mo-old and 24-mo-old rats had higher expression levels compared with 3-mo rats ($P < 0.05$). There were no between group differences for L1.Tot DNA content (Fig. 1F) or nuclear ORF1 protein expression (Fig. 1I).

RNA-Sequencing Results Between 3-Mo-Old and 24-Mo-Old Rats for Generating Downstream Assays

Upon receiving RNA-sequencing results, we aimed to examine the mRNA expression patterns of genes related to LINE-1 regulation from previous literature (50). In the first cluster of genes, LINE-1 transcriptional activators (Fig. 2A), *Hdac2* was significantly lower in 24- compared with 3-mo rats ($P = 0.007$). Additionally, *Ctcf*, *Klf4*, and *Elf1* were significantly higher in 24- compared with 3-mo rodents ($P < 0.05$ for each target). In the second cluster of genes, endogenous LINE-1 inhibitors (Fig. 2B), *Cdkn1a* was significantly higher in 24- compared with 3-mo rodents ($P = 0.003$). In the third cluster of genes, or genes related to DNA methylation (Fig. 2C), *Tet1* was significantly lower in 24- compared with 3-mo rodents ($P < 0.001$).

Effect of Aging on Skeletal Muscle L1.3 DNA Methylation, L1.3 DNA Accessibility, Global DNMT Activity, and Global HDAC Activity

L1.3 DNA methylation and expression values of L1.3 DNA in the euchromatin state were not normally distributed and these variables were log-transformed before statistical analysis. There were no between-group differences for L1.3 5'-UTR DNA methylation ($P = 0.160$, $\eta_p^2 = 0.16$; Fig. 3A) or L1.3

DNA in the euchromatin state ($P = 0.150$, $\eta_p^2 = 0.17$; Fig. 3B), although a forced post hoc indicated that this variable was greater in 24-mo-old versus 3-mo-old rats. Nuclear DNMT activity was statistically significantly different between age groups ($P = 0.018$, $\eta_p^2 = 0.32$; Fig. 3C), and post hoc analysis revealed that both 12-mo-old and 24-mo-old rats possessed lower nuclear DNMT activity compared with 3-mo-old rats ($P = 0.016$). Nuclear DNMT3A protein expression was statistically significant ($P < 0.001$, $\eta_p^2 = 0.48$; Fig. 3E), and post hoc analysis revealed that both 12-mo-old and 24 mo-old rats possessed paradoxically higher nuclear DNMT3A protein expression compared with 3-mo-old rats ($P < 0.05$). No differences between groups existed for nuclear TET1 protein expression (Fig. 3F). Notably, we attempted to probe for nuclear CTCF and HDAC2 protein expression, but no signals were detected in the nuclear fraction (data not shown).

DISCUSSION

This is the first investigation examining skeletal muscle LINE-1 mRNA and DNA expression across the age spectrum in rats. Our observations of higher LINE-1 mRNA and genomic DNA expression in older versus younger rats is in agreement with our hypotheses as well as the findings of De Cecco et al. (8) who previously reported skeletal muscle LINE-1 mRNA and DNA copy number were higher in 36-mo-old versus 5-mo-old mice.

Skeletal muscle aging in rodents and humans is largely conserved, and involves a reduction in fiber size and number of type II fibers, a loss in resident satellite cells, a dysfunction in translational machinery, a decrease in contractile protein con-

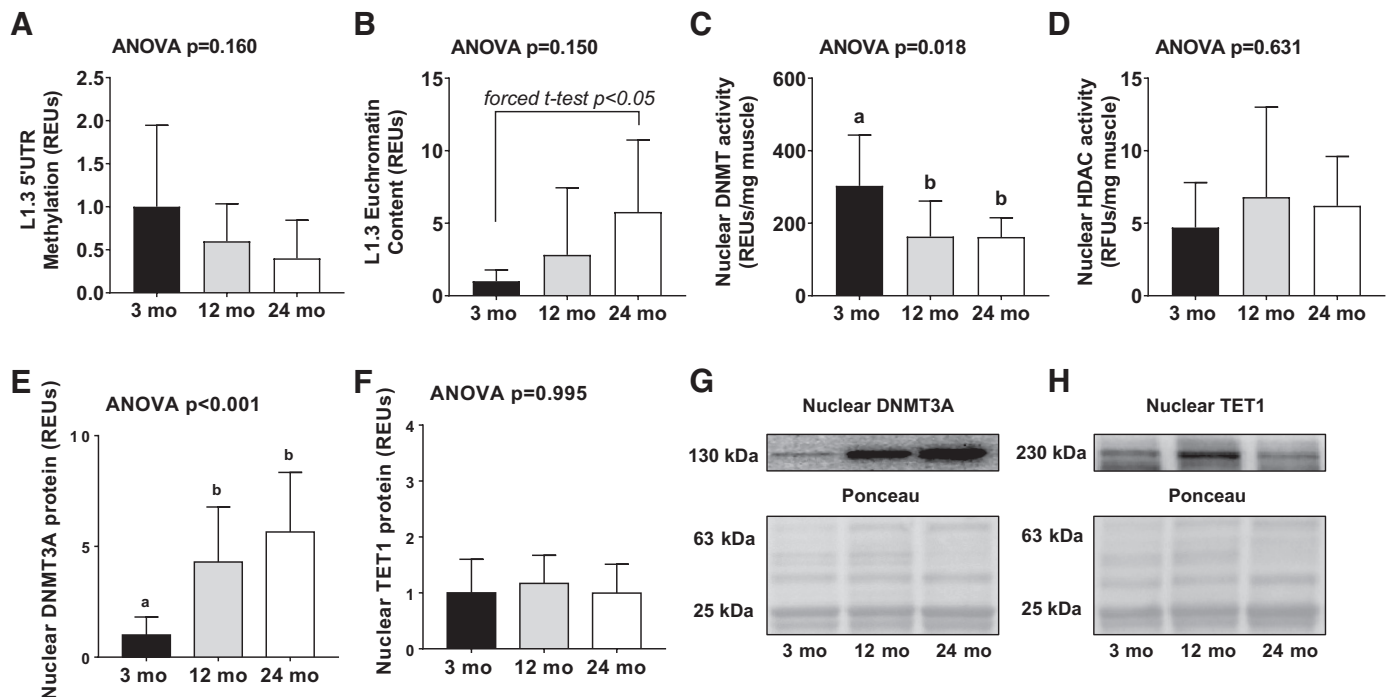


Fig. 3. Effect of aging on skeletal muscle long interspersed element-1 (LINE-1) 5'-UTR (5' untranslated region) methylation and chromatin accessibility. A: age group differences in L1.3 5'-UTR methylation ($n = 8$ per group). B: L1.3 euchromatin content ($n = 8$ per group). C: nuclear DNA methyltransferase (DNMT) activity ($n = 8$ per group). D: nuclear histone deacetylase (HDAC) activity ($n = 8$ per group). E: nuclear DNMT3a protein expression ($n = 9$ per group). F: nuclear TET1 protein expression ($n = 8$ per group). G and H: representative Western blot images. REU, relative expression units. Data are means \pm SD. ^{a,b}Significant between-group age differences ($P < 0.05$).

tent, an increase in fibrotic tissue, and a decrease in mitochondrial function (reviewed in Ref. 36). Indeed, a major limitation of this study is that we did not observe lower contractile protein concentrations or citrate synthase activity levels (reflective of mitochondrial content and function) in the 24-mo-old rats versus other groups. However, we did observe that gastrocnemius muscle weights, both on an absolute and relative scale, were lower in 24-mo versus 12-mo rats. This age-related atrophy may reflect the beginnings of muscle aging and, had we examined older animals, we likely would have captured a more egregious muscle-aging phenotype.

While the mechanistic causes of muscle aging are multifactorial, three intriguing molecular signatures of muscle aging in rodents and humans exist including: 1) transcriptome-wide changes in mRNA expression (35, 43), 2) genome-wide alterations in DNA methylation patterns, which, in turn, likely contribute to said transcriptome changes (56), and 3) an alteration in mRNA splicing, which leads to the formation of more transcript variants (46). It seems reasonable to speculate that these age-associated nuclear genome alterations likely contribute to muscle aging from a top down perspective; that is, a dysregulation in mRNA expression may lead to altered expression of critical proteins and enzymes needed to maintain cellular homeostasis. Given that LINE-1 retrotransposition has the ability to disrupt the genetic code and affect global transcriptome-wide patterns, the notion that increased skeletal muscle LINE-1 retrotransposition during aging is partially, if not predominantly, responsible for the aforementioned genome- or transcriptome-wide alterations is an attractive hypothesis.

We attempted to elucidate biomarkers which potentially explains how aging increases skeletal muscle LINE-1 activity. RNA-sequencing indicated mRNAs for *Hdac2*, which encodes for a histone deacetylase enzyme, and *Tet1*, which encodes for an enzyme that affects DNA methylation, were both significantly lower in the older versus younger cohort. L1.3 DNA chromatin accessibility also increased across the age spectrum and was significantly higher in older versus younger rats. Collectively these data suggest that age-related decrements in chromatin modifying enzymes, or systems at large, may alter chromatin structure to expose more LINE-1 copies for transcription. However, nuclear fraction experiments proved difficult in validating this hypothesis. First, nuclear DNMT3A protein was paradoxically higher in older rats, and nuclear TET1 protein levels were not different between age groups. Additionally, while we attempted to probe for nuclear HDAC2 protein, we discovered that it was likely too low as expressed to be detected using conventional Western blot analysis techniques. Finally, nuclear HDAC activity was not different between age groups. One intriguing finding, which did seem to support our hypothesis, however, is that nuclear DNMT activity was lower in the 12-mo-old and 24-mo-old versus 3-mo-old rats despite older rats possessing greater levels of nuclear DNMT3A protein. Discordant findings between higher DNMT3A protein and lower DNMT activity in older rats is difficult to reconcile, although it may be due to a feedback mechanism in an attempt to increase DNMT activity. Notwithstanding, age-related decrements in DNMT activity may be a mechanism that alters chromatin to expose more active LINE-1-containing DNA regions. These phenomena, in turn, may lead to the upregulation in LINE-1 mRNA expres-

sion and eventual increase in de novo LINE-1 integration; both of which were observed in the older versus younger rats herein. This working model agrees with De Cecco et al. (8) who posited that there is a loosening of specific LINE-1 genomic regions in postmitotic skeletal muscle fibers with aging, and this phenomenon leads to increases in LINE-1 mRNA expression and LINE-1 genomic insertions.

One final topic critical to this discussion is the ramifications of increased skeletal muscle LINE-1 activity with aging. LINE-1 retrotransposition has been associated with >100 different diseases ranging from Duchene muscular dystrophy, hemophilia, neurofibromatosis, and various cancers (16), and recent estimates suggest LINE-1-mediated retrotransposition events account for ~1 of every 1,000 spontaneous and disease-producing insertions in humans (4). LINE-1 transcripts have also been shown to be upregulated in synovial fluid samples obtained from patients suffering from rheumatoid arthritis (40), and others have reported that a robust elevation in LINE-1 mRNA expression levels occurs following ischemia-reperfusion in rat cardiac tissue (29). As mentioned, it is also notable that global Sirt6-knockout mice demonstrated enhanced global LINE-1 mRNA expression as well as lower muscle masses and quadriceps muscle fiber diameters compared with wild-type mice (49). Therefore, while we did not decipher whether increased skeletal muscle LINE-1 activity coincides with or causes muscle aging, we maintain the hypothesis that increased LINE-1 activity with aging is likely disruptive to cellular homeostasis and this needs to be more firmly established in future research endeavors.

Perspectives and Significance

In conclusion, this is the first observation of higher skeletal muscle LINE-1 mRNA and DNA expression in older versus younger rats. We posit that these observations are potentially due to increased LINE-1 DNA accessibility across the age span. Increased tissue LINE-1 activity with aging is generally viewed as negative due to the increased mutagenic potential that may be caused through retrotransposition. Therefore, future research is needed to investigate how increases in LINE-1 mRNA and DNA expression affects skeletal muscle physiology, and if this pathway appreciably contributes to the skeletal muscle aging process.

ACKNOWLEDGMENTS

We thank Dr. John J. McCarthy (University of Kentucky) for his intellectual insight.

Readers seeking to obtain the RNA-seq data from this study can email the corresponding author. All raw data are available upon request by contacting the corresponding author.

DISCLOSURES

Reagents for this study were purchased through discretionary laboratory funds of M. D. Roberts. No conflicts of interest, financial or otherwise, are declared by the authors.

AUTHOR CONTRIBUTIONS

P.W.M., M.A.R., and M.D.R. conceived and designed research; P.W.M., M.A.R., S.C.O., P.A.R., and C.B.M. performed experiments; P.W.M., M.A.R., A.N.K., and M.D.R. analyzed data; P.W.M., M.A.R., S.C.O., P.A.R., C.G.V., M.D.B., A.N.K., K.C.Y., and M.D.R. interpreted results of experiments; P.W.M. and M.D.R. prepared figures; P.W.M. drafted manuscript; P.W.M., M.A.R., S.C.O., P.A.R., C.G.V., C.B.M., M.D.B., A.N.K., K.C.Y., and M.D.R. edited and revised manuscript; P.W.M., M.A.R., S.C.O., P.A.R., C.G.V.,

C.B.M., M.D.B., A.N.K., K.C.Y., and M.D.R. approved final version of manuscript.

REFERENCES

- Balagopal P, Rooyackers OE, Adey DB, Ades PA, Nair KS. Effects of aging on in vivo synthesis of skeletal muscle myosin heavy-chain and sarcoplasmic protein in humans. *Am J Physiol Endocrinol Metab* 273: E790–E800, 1997. doi:10.1152/ajpendo.1997.273.4.E790.
- Balagopal P, Schimke JC, Ades P, Adey D, Nair KS. Age effect on transcript levels and synthesis rate of muscle MHC and response to resistance exercise. *Am J Physiol Endocrinol Metab* 280: E203–E208, 2001. doi:10.1152/ajpendo.2001.280.2.E203.
- Beck CR, Collier P, Macfarlane C, Malig M, Kidd JM, Eichler EE, Badge RM, Moran JV. LINE-1 retrotransposition activity in human genomes. *Cell* 141: 1159–1170, 2010. doi:10.1016/j.cell.2010.05.021.
- Beck CR, Garcia-Perez JL, Badge RM, Moran JV. LINE-1 elements in structural variation and disease. *Annu Rev Genomics Hum Genet* 12: 187–215, 2011. doi:10.1146/annurev-genom-082509-141802.
- Brocca L, McPhee JS, Longa E, Canepari M, Seynnes O, De Vito G, Pellegrino MA, Narici M, Bottinelli R. Structure and function of human muscle fibres and muscle proteome in physically active older men. *J Physiol* 595: 4823–4844, 2017. doi:10.1113/JP274148.
- Cohen S, Brault JJ, Gygi SP, Glass DJ, Valenzuela DM, Gartner C, Latres E, Goldberg AL. During muscle atrophy, thick, but not thin, filament components are degraded by MuRF1-dependent ubiquitylation. *J Cell Biol* 185: 1083–1095, 2009. doi:10.1083/jcb.200901052.
- Cost GJ, Feng Q, Jacquier A, Boeke JD. Human L1 element target-primed reverse transcription in vitro. *EMBO J* 21: 5899–5910, 2002. doi:10.1093/emboj/cdf592.
- De Cecco M, Criscione SW, Peterson AL, Neretti N, Sedivy JM, Kreiling JA. Transposable elements become active and mobile in the genomes of aging mammalian somatic tissues. *Aging (Albany NY)* 5: 867–883, 2013. doi:10.18632/aging.100621.
- Doucet AJ, Hulme AE, Sahinovic E, Kulpa DA, Moldovan JB, Kopera HC, Athanikar JN, Hasnaoui M, Bucheton A, Moran JV, Gilbert N. Characterization of LINE-1 ribonucleoprotein particles. *PLoS Genet* 6: e1001150, 2010. doi:10.1371/journal.pgen.1001150.
- Feng Q, Moran JV, Kazazian HH Jr, Boeke JD. Human L1 retrotransposon encodes a conserved endonuclease required for retrotransposition. *Cell* 87: 905–916, 1996. doi:10.1016/S0092-8674(00)81997-2.
- Frazee AC, Perteza G, Jaffe AE, Langmead B, Salzberg SL, Leek JT. Ballgown bridges the gap between transcriptome assembly and expression analysis. *Nat Biotechnol* 33: 243–246, 2015. doi:10.1038/nbt.3172.
- Gasior SL, Wakeman TP, Xu B, Deininger PL. The human LINE-1 retrotransposon creates DNA double-strand breaks. *J Mol Biol* 357: 1383–1393, 2006. doi:10.1016/j.jmb.2006.01.089.
- Gibbs RA, Weinstock GM, Metzker ML, Muzny DM, Sodergren EJ, Scherer S, Scott G, Steffen D, Worley KC, Burch PE, Okwuonu G, Hines S, Lewis L, DeRamo C, Delgado O, Dugan-Rocha S, Miner G, Morgan M, Hawes A, Gill R, Celera, Holt RA, Adams MD, Amanatides PG, Baden-Tillson H, Barnstead M, Chin S, Evans CA, Ferreria S, Foslter C, Glodek A, Gu Z, Jennings D, Kraft CL; Rat Genome Sequencing Project Consortium. Genome sequence of the Brown Norway rat yields insights into mammalian evolution. *Nature* 428: 493–521, 2004. doi:10.1038/nature02426.
- Goodier JL, Ostertag EM, Du K, Kazazian HH Jr. A novel active L1 retrotransposon subfamily in the mouse. *Genome Res* 11: 1677–1685, 2001. doi:10.1101/gr.198301.
- Haddad F, Adams GR. Aging-sensitive cellular and molecular mechanisms associated with skeletal muscle hypertrophy. *J Appl Physiol (1985)* 100: 1188–1203, 2006. doi:10.1152/jappphysiol.01227.2005.
- Hancks DC, Kazazian HH Jr. Active human retrotransposons: variation and disease. *Curr Opin Genet Dev* 22: 191–203, 2012. doi:10.1016/j.gde.2012.02.006.
- Haus JM, Carrithers JA, Trappe SW, Trappe TA. Collagen, cross-linking, and advanced glycation end products in aging human skeletal muscle. *J Appl Physiol (1985)* 103: 2068–2076, 2007. doi:10.1152/jappphysiol.00670.2007.
- Hohjoh H, Singer MF. Cytoplasmic ribonucleoprotein complexes containing human LINE-1 protein and RNA. *EMBO J* 15: 630–639, 1996. doi:10.1002/j.1460-2075.1996.tb00395.x.
- Hyatt HW, Kephart WC, Holland AM, Mumford P, Mobley CB, Lowery RP, Roberts MD, Wilson JM, Kavazis AN. A ketogenic diet in rodents elicits improved mitochondrial adaptations in response to resistance exercise training compared to an isocaloric Western diet. *Front Physiol* 7: 1–9, 2016. doi:10.3389/fphys.2016.00533.
- Jakobsson F, Borg K, Edström L, Grimby L. Use of motor units in relation to muscle fiber type and size in man. *Muscle Nerve* 11: 1211–1218, 1988. doi:10.1002/mus.880111205.
- Johnson ML, Robinson MM, Nair KS. Skeletal muscle aging and the mitochondrion. *Trends Endocrinol Metab* 24: 247–256, 2013. doi:10.1016/j.tem.2012.12.003.
- Kim D, Langmead B, Salzberg SL. HISAT: a fast spliced aligner with low memory requirements. *Nat Methods* 12: 357–360, 2015. doi:10.1038/nmeth.3317.
- Kirilyuk A, Tolstogon GV, Damert A, Held U, Hahn S, Löwer R, Buschmann C, Horn AV, Traub P, Schumann GG. Functional endogenous LINE-1 retrotransposons are expressed and mobilized in rat chloroleukemia cells. *Nucleic Acids Res* 36: 648–665, 2008. doi:10.1093/nar/gkm1045.
- Lander ES, Linton LM, Birren B, Nusbaum C, Zody MC, Baldwin J, Devon K, Dewar K, Doyle M, FitzHugh W, Funke R, Gage D, Harris K, Heaford A, Howland J, Kann L, Lehoczky J, LeVine R, McEwan P, McKernan K, Meldrim J, Mesirov JP, Miranda C, Morris V, Naylor J, Raymond C, Rosetti M, Santos R, Sheridan A, Sougnez C, Stange-Thomann Y, Stojanovic N, Subramanian A, Wyman D; International Human Genome Sequencing Consortium. Initial sequencing and analysis of the human genome. *Nature* 409: 860–921, 2001. [Erratum in *Nature* 411: 720, 2001; 412: 565, 2001.] doi:10.1038/35057062.
- Larsson L, Degens H, Li M, Salvati L, Lee YI, Thompson W, Kirkland JL, Sandri M. Sarcopenia: aging-related loss of muscle mass and function. *Physiol Rev* 99: 427–511, 2019. doi:10.1152/physrev.00061.2017.
- Larsson L, Sjödin B, Karlsson J. Histochemical and biochemical changes in human skeletal muscle with age in sedentary males, age 22–65 years. *Acta Physiol Scand* 103: 31–39, 1978. doi:10.1111/j.1748-1716.1978.tb06187.x.
- López-Otín C, Blasco MA, Partridge L, Serrano M, Kroemer G. The hallmarks of aging. *Cell* 153: 1194–1217, 2013. doi:10.1016/j.cell.2013.05.039.
- Luan DD, Korman MH, Jakubczak JL, Eickbush TH. Reverse transcription of R2Bm RNA is primed by a nick at the chromosomal target site: a mechanism for non-LTR retrotransposition. *Cell* 72: 595–605, 1993. doi:10.1016/0092-8674(93)90078-5.
- Lucchinetti E, Feng J, Silva R, Tolstogon GV, Schaub MC, Schumann GG, Zaugg M. Inhibition of LINE-1 expression in the heart decreases ischemic damage by activation of Akt/PKB signaling. *Physiol Genomics* 25: 314–324, 2006. doi:10.1152/physiolgenomics.00251.2005.
- Martin M. Cutadapt removes adapter sequences from high-throughput sequencing reads. *EMBnet journal* 17: 10–12, 2011. doi:10.14806/ej.17.1.200.
- Martin SL. Ribonucleoprotein particles with LINE-1 RNA in mouse embryonal carcinoma cells. *Mol Cell Biol* 11: 4804–4807, 1991. doi:10.1128/MCB.11.9.4804.
- Martin SL, Branciforte D, Keller D, Bain DL. Trimeric structure for an essential protein in L1 retrotransposition. *Proc Natl Acad Sci USA* 100: 13815–13820, 2003. doi:10.1073/pnas.2336221100.
- Marx JO, Kraemer WJ, Nindl BC, Larsson L. Effects of aging on human skeletal muscle myosin heavy-chain mRNA content and protein isoform expression. *J Gerontol A Biol Sci Med Sci* 57: B232–B238, 2002. doi:10.1093/gerona/57.6.B232.
- Mathias SL, Scott AF, Kazazian HH Jr, Boeke JD, Gabriel A. Reverse transcriptase encoded by a human transposable element. *Science* 254: 1808–1810, 1991. doi:10.1126/science.1722352.
- Melov S, Tarnopolsky MA, Beckman K, Felkey K, Hubbard A. Resistance exercise reverses aging in human skeletal muscle. *PLoS One* 2: e465, 2007. doi:10.1371/journal.pone.0000465.
- Miljkovic N, Lim JY, Miljkovic I, Frontera WR. Aging of skeletal muscle fibers. *Ann Rehabil Med* 39: 155–162, 2015. doi:10.5535/arm.2015.39.2.155.
- Mobley CB, Mumford PW, Kephart WC, Haun CT, Holland AM, Beck DT, Martin JS, Young KC, Anderson RG, Patel RK, Langston GL, Lowery RP, Wilson JM, Roberts MD. Aging in rats differentially affects markers of transcriptional and translational capacity in soleus and plantaris muscle. *Front Physiol* 8: 1–13, 2017. doi:10.3389/fphys.2017.00518.
- Monemi M, Eriksson PO, Eriksson A, Thornell LE. Adverse changes in fibre type composition of the human masseter versus biceps brachii

- muscle during aging. *J Neurol Sci* 154: 35–48, 1998. doi:10.1016/S0022-510X(97)00208-6.
39. Mumford PW, Romero MA, Mao X, Mobley CB, Kephart WC, Haun CT, Roberson PA, Young KC, Martin JS, Yarrow JF, Beck DT, Roberts MD. Cross talk between androgen and Wnt signaling potentially contributes to age-related skeletal muscle atrophy in rats. *J Appl Physiol (1985)* 125: 486–494, 2018. doi:10.1152/jappphysiol.00768.2017.
 40. Neidhart M, Rethage J, Kuchen S, Künzler P, Crowl RM, Billingham ME, Gay RE, Gay S. Retrotransposable L1 elements expressed in rheumatoid arthritis synovial tissue: association with genomic DNA hypomethylation and influence on gene expression. *Arthritis Rheum* 43: 2634–2647, 2000. doi:10.1002/1529-0131(200012)43:12<2634::AID-ANR3>3.0.CO;2-1.
 41. Penzkofer T, Jäger M, Figlerowicz M, Badge R, Mundlos S, Robinson PN, Zemotjel T. L1Base 2: more retrotransposition-active LINE-1s, more mammalian genomes. *Nucleic Acids Res* 45: D68–D73, 2017. doi:10.1093/nar/gkw925.
 42. Perteu M, Perteu GM, Antonescu CM, Chang T-C, Mendell JT, Salzberg SL. StringTie enables improved reconstruction of a transcriptome from RNA-seq reads. *Nat Biotechnol* 33: 290–295, 2015. doi:10.1038/nbt.3122.
 - 42a. R Core Team. *R: A Language and Environment for Statistical Computing*. Vienna, Austria: R Foundation for Statistical Computing, 2013. https://www.r-project.org/.
 43. Raue U, Trappe TA, Estrem ST, Qian HR, Helvering LM, Smith RC, Trappe S. Transcriptome signature of resistance exercise adaptations: mixed muscle and fiber type specific profiles in young and old adults. *J Appl Physiol (1985)* 112: 1625–1636, 2012. doi:10.1152/jappphysiol.00435.2011.
 44. Richardson SR, Doucet AJ, Kopera HC, Moldovan JB, Garcia-Perez JL, Moran JV. The influence of LINE-1 and SINE retrotransposons on mammalian genomes. *Microbiol Spectr* 3: A3–A0061, 2015. doi:10.1128/microbiolspec.MDNA3-0061-2014.
 45. Roberts MD, Romero MA, Mobley CB, Mumford PW, Roberson PA, Haun CT, Vann CG, Osburn SC, Holmes HH, Greer RA, Lockwood CM, Parry HA, Kavazis AN. Skeletal muscle mitochondrial volume and myozenin-1 protein differences exist between high versus low anabolic responders to resistance training. *PeerJ* 6: e5338, 2018. doi:10.7717/peerj.5338.
 46. Rodríguez SA, Grochová D, McKenna T, Borate B, Trivedi NS, Erdos MR, Eriksson M. Global genome splicing analysis reveals an increased number of alternatively spliced genes with aging. *Aging Cell* 15: 267–278, 2016. doi:10.1111/accel.12433.
 - 46a. RStudio. *RStudio: Integrated Development for R*. Boston, MA: RStudio, 2015. https://www.rstudio.com/.
 47. Scelsi R, Marchetti C, Poggi P. Histochemical and ultrastructural aspects of m. vastus lateralis in sedentary old people (age 65–89 years). *Acta Neuropathol* 51: 99–105, 1980. doi:10.1007/BF00690450.
 48. Short KR, Vittone JL, Bigelow ML, Proctor DN, Coenen-Schimke JM, Rys P, Nair KS. Changes in myosin heavy chain mRNA and protein expression in human skeletal muscle with age and endurance exercise training. *J Appl Physiol (1985)* 99: 95–102, 2005. doi:10.1152/jappphysiol.00129.2005.
 49. Simon M, Van Meter M, Ablaeva J, Ke Z, Gonzalez RS, Taguchi T, De Cecco M, Leonova KI, Kogan V, Helfand SL, Neretti N, Roichman A, Cohen HY, Meer MV, Gladyshev VN, Antoch MP, Gudkov AV, Sedivy JM, Seluanov A, Gorbunova V. LINE1 derepression in aged wild-type and SIRT6-deficient mice drives inflammation. *Cell Metab* 29: 871–885.e5, 2019. doi:10.1016/j.cmet.2019.02.014.
 50. Sun X, Wang X, Tang Z, Grivainis M, Kahler D, Yun C, Mita P, Fenyö D, Boeke JD. Transcription factor profiling reveals molecular choreography and key regulators of human retrotransposon expression. *Proc Natl Acad Sci USA* 115: E5526–E5535, 2018. doi:10.1073/pnas.1722565115.
 53. Van Meter M, Kashyap M, Rezazadeh S, Geneva AJ, Morello TD, Seluanov A, Gorbunova V. SIRT6 represses LINE1 retrotransposons by ribosylating KAP1 but this repression fails with stress and age. *Nat Commun* 5: 5011, 2014. doi:10.1038/ncomms6011.
 54. Waterston RH, Lindblad-Toh K, Birney E, Rogers J, Abril JF, Agarwal P, Agarwala R, Ainscough R, Alexandersson M, An P, Antonarakis SE, Attwood J, Baertsch R, Bailey J, Barlow K, Beck S, Berry E, Birren B, Bloom T, Bork P, Botcherby M, Bray N, Brent MR, Brown DG, Brown SD, Bult C, Burton J, Butler J, Campbell RD, Carninci P, Cawley S, Chiaromonte F, Chinwalla AT, Church DM; Mouse Genome Sequencing Consortium. Initial sequencing and comparative analysis of the mouse genome. *Nature* 420: 520–562, 2002. doi:10.1038/nature01262.
 55. Wei W, Gilbert N, Ooi SL, Lawler JF, Ostertag EM, Kazazian HH, Boeke JD, Moran JV. Human L1 retrotransposition: cis preference versus trans complementation. *Mol Cell Biol* 21: 1429–1439, 2001. doi:10.1128/MCB.21.4.1429-1439.2001.
 56. Zykovich A, Hubbard A, Flynn JM, Tarnopolsky M, Fraga MF, Kerkick C, Ogborn D, MacNeil L, Mooney SD, Melov S. Genome-wide DNA methylation changes with age in disease-free human skeletal muscle. *Aging Cell* 13: 360–366, 2014. doi:10.1111/accel.12180.